

**Magnetic characteristics of nanocrystalline multiferroic BiFeO<sub>3</sub> at low temperatures**

S. Vijayanand, M. B. Mahajan, H. S. Potdar, and P. A. Joy\*

*Physical and Materials Chemistry Division, National Chemical Laboratory, Pune 411008, India*

(Received 17 March 2009; revised manuscript received 10 August 2009; published 27 August 2009)

The magnetic characteristics of nanocrystalline BiFeO<sub>3</sub> with average crystallite sizes of  $\sim 50$  and  $\sim 100$  nm are evaluated by studying the temperature and field dependence of magnetization at low temperatures. Different properties such as magnetization, coercivity, and remanence show evidence for changes in the magnetic properties associated with the phase transitions at low temperatures, reported from Raman studies. Detailed field-cooled and zero-field-cooled magnetization measurements show that the likely origin of the changes in the magnetic characteristics is from the changes in the domain structure.

DOI: [10.1103/PhysRevB.80.064423](https://doi.org/10.1103/PhysRevB.80.064423)

PACS number(s): 75.50.-y, 75.60.-d, 75.75.+a

**I. INTRODUCTION**

The single phase multiferroic material BiFeO<sub>3</sub> has received considerable attention recently because of its very interesting magnetoelectric properties for spintronic applications.<sup>1</sup> BiFeO<sub>3</sub> is antiferromagnetic below  $T_N=643$  K and shows ferroelectric behavior below  $T_C=1100$  K so that the material exhibits multiferroic properties at room temperature.<sup>2</sup> The magnetic structure of BiFeO<sub>3</sub> is of *G*-type antiferromagnetic, with a modulated spiral spin structure having a long periodicity of 62 nm.<sup>3</sup> Recent neutron-diffraction studies revealed that the character of the modulated cycloidal ordering of the Fe<sup>3+</sup> magnetic moments remains the same from 4 K up to the Neel temperature, suggesting that the magnetic interactions are relatively stable in this temperature range.<sup>4</sup> Similarly, high-resolution synchrotron-radiation diffraction did not show any sign of charge ordering nor any crystal symmetry breaking in BiFeO<sub>3</sub> in the temperature range 5–1000 K.<sup>5</sup>

Zero-field-cooled (ZFC) and field-cooled (FC) magnetization studies on single crystals, in a field of 10 kOe, showed a decrease below 350 K like a conventional antiferromagnet but the two curves diverge below 250 K, indicating spin-glass behavior.<sup>6</sup> However, further studies on thin films reported a spin-glass transition at 50 K.<sup>7</sup> Recent studies indicated few more weak magnetic transitions below and above room temperature. A ferromagnetic phase transition is observed at 150 K from studies on (001) and (110) oriented thin films.<sup>8</sup> From the studies on the temperature dependence of the Raman integrated intensities of the electromagnon on single crystals of BiFeO<sub>3</sub>, a maximum around 140 K is observed, indicating a small spin reorientation out of the cycloidal plane.<sup>9</sup> Phase transitions at 90, 140, 200, and 250 K are discovered from Raman spectroscopic studies.<sup>10</sup> These transitions are also observed in dielectric constant measurements and thermomechanical studies.<sup>11</sup> The transitions are assigned to different origins such as magnetic but glassy and with magnetoelectric coupling phase transition at 50 K, dominantly magnetic transition at 140 K, magnetoelastic phase transition at 200 K, and magnetic but glassy transition at 230 K.

Studies on nanosized BiFeO<sub>3</sub> have gained momentum recently because of the possibility of inducing ferromagnetism in the material at room temperature by decreasing the par-

ticule size. A high magnetic moment of  $0.4\mu_B/\text{Fe}$  is reported for nanoparticles of size  $\sim 4$  nm when compared to the value of  $0.02\mu_B/\text{Fe}$  for the bulk material.<sup>12</sup> From the studies on the size-dependent magnetic properties, Park *et al.* showed that the spiral spin structure is suppressed with decreasing particle size.<sup>13</sup> A spin-glass freezing behavior is observed for the nanoparticles due to the interplay between size effects, interparticle interactions, and random distribution of anisotropy axes. In this paper, we report the magnetic characteristics of nanocrystalline BiFeO<sub>3</sub>, of size  $\sim 50$  nm and  $\sim 100$  nm, at low temperatures and show that some anomalies are observed at different temperatures corresponding to the different phase transitions discovered from Raman and other studies.

**II. EXPERIMENT**

Nanocrystalline BiFeO<sub>3</sub> was synthesized by a coprecipitation method using aqueous solutions of Bi(NO<sub>3</sub>)<sub>3</sub>·5H<sub>2</sub>O (0.05 M), Fe(NO<sub>3</sub>)<sub>3</sub>·9H<sub>2</sub>O (0.05 M), and K<sub>2</sub>CO<sub>3</sub> (0.6 M). The precipitate formed was digested at 70 °C for 2 h. Finally, the precipitate was washed with deionized water to avoid potassium ion contamination and then dried overnight in an oven. The dried powder was calcined initially at 500 °C (sample code: BF500) and part of the sample was further calcined at 650 °C (sample code: BF650) for 3 h each. The calcined samples were characterized for phase purity by powder x-ray diffraction (XRD) (using Cu *K*α radiation, Ni filter) using a Philips X'pert Pro powder x-ray diffractometer. Magnetic measurements below 300 K were performed on a vibrating sample magnetometer in a physical property measuring system (PPMS) of Quantum Design and using a PAR EG&G 4500 vibrating sample magnetometer above 300 K.

**III. RESULTS AND DISCUSSION**

Figure 1 shows the powder x-ray diffraction patterns of the calcined samples compared to the simulated pattern of BiFeO<sub>3</sub>. The powder pattern is simulated using the rhombohedral space group *R3c* and the corresponding hexagonal lattice parameters  $a=5.5810$  Å and  $c=13.8685$  Å. The lattice parameters of the two samples calculated by least-squares refinement of the diffraction patterns are found to be

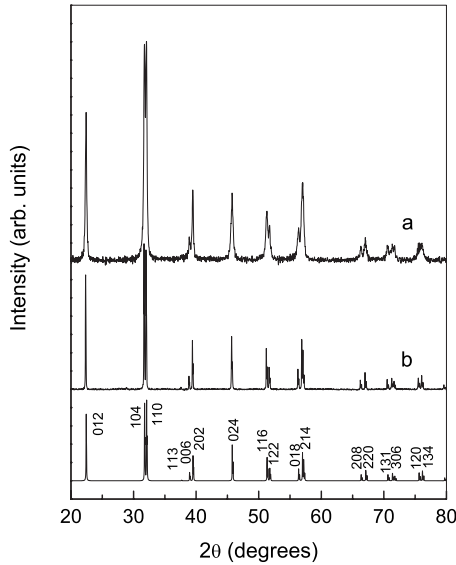


FIG. 1. Powder XRD patterns of (a) BF500 and (b) BF650. The simulated pattern of  $\text{BiFeO}_3$  is indexed and shown at the bottom for comparison.

comparable to the values reported for single crystalline  $\text{BiFeO}_3$ . All the reflections in the XRD pattern of BF500 are broad due to the nanocrystalline nature of the sample synthesized at low temperatures. The average crystallite size is calculated from x-ray line broadening using the Scherrer formula,  $D=0.9\lambda/\beta \cos \theta$ , where  $D$  is the crystallite size in Å,  $\beta$  is the half maximum line width corrected for instrumental line broadening, and  $\lambda$  is the wavelength of x rays. The crystallite size is obtained as 48 nm for BF500 and as 97 nm for BF650.

To confirm the single phase nature of the nanocrystalline  $\text{BiFeO}_3$ , magnetic measurements were performed above room temperature. FC and ZFC magnetization curves of BF500 above 300 K are shown in Fig. 2. The magnetization curves show a magnetic transition below 650 K, indicating that the sample becomes ferromagnetic at the Neel temperature of  $\text{BiFeO}_3$  (643 K). The divergence between FC and

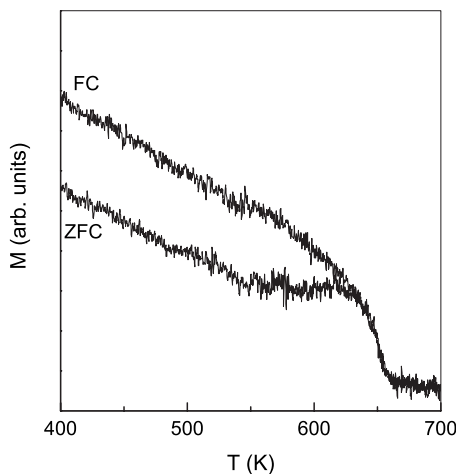


FIG. 2. FC and ZFC magnetization curves of BF500 above room temperature.

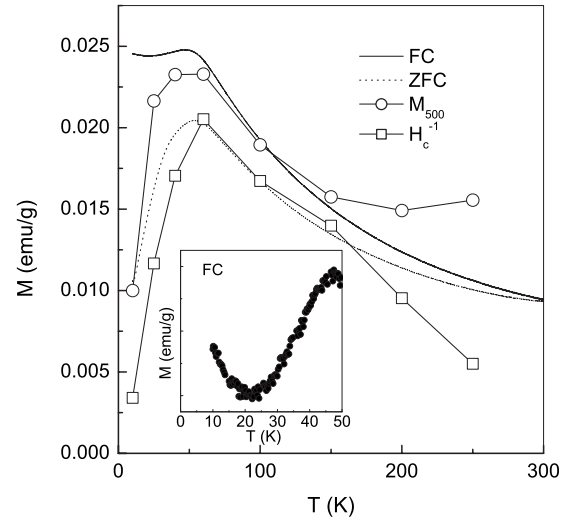


FIG. 3. FC and ZFC magnetization curves of BF500 measured in a field of 500 Oe. The circles correspond to the magnetization at 500 Oe extracted from the initial magnetization measured at different temperatures. The squares are the inverse of the coercivity at different temperatures normalized to the maximum in the ZFC curve. Inset: enlarged FC curve in the 10–50 K region.

ZFC magnetization curves below 640 K is similar to that found for other ferro- and ferrimagnetic materials.<sup>14</sup> These results suggest that BF500 is single-phase  $\text{BiFeO}_3$  and that it becomes ferromagnetic when the particle size is reduced.

ZFC and FC magnetization curves of BF500 below 300 K are shown in Fig. 3. Deviation between the FC and ZFC magnetizations is observed below 300 K. A broad maximum is observed at 53 K in the ZFC magnetization curve. The FC magnetization decreases initially with increasing temperature and after going through a minimum at 22 K, a maximum is reached at 47 K and the magnetization decreases again at higher temperatures. For BF650, the FC and ZFC curves [see Fig. 7(b)] deviate below 230 K and show further enlarged deviation with a slope change below 150 K. Both curves show a large increase in the magnetization below 23 K.

Initial magnetization curves of BF500 measured at different temperatures, shown in Fig. 4, give more information on the changes in the magnetic characteristics of the sample at low temperatures. As the magnetization is not saturated, the saturation magnetization is obtained by extrapolating the  $M$  vs  $1/H$  curve to  $1/H=0$ . At 10 K, the magnetization is very low at low fields whereas higher magnetization is observed in the 25–75 K region. It is known that the initial magnetization curve reflects the domain pinning effects of a magnetic system and the same is reflected in the shape of the ZFC magnetization curves.<sup>15</sup> A comparison of the initial magnetization at 500 Oe as a function of temperature is compared to the ZFC magnetization measured at 500 Oe in Fig. 3. Apart from a maximum at 50 K, a minimum is observed at 200 K in the initial magnetization recorded at 500 Oe. The shapes of both curves are almost similar, except for the larger values of  $M_{500}$  extracted from the initial magnetization curves. This is possibly due to the fact that there was a small remanent magnetization after the measurements at the successive low temperatures.

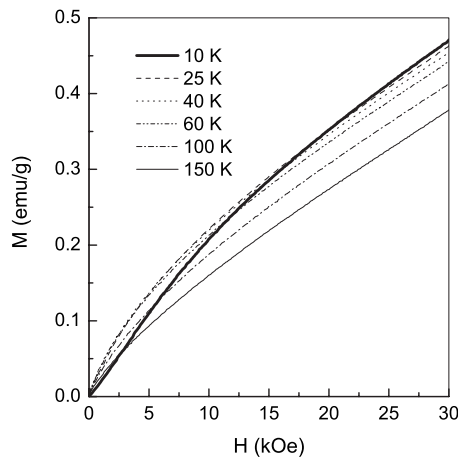


FIG. 4. Initial magnetization of BF500 measured at different temperatures.

Figure 5 shows the magnetic hysteresis curves of BF500 measured at different temperatures in the range 10–300 K. The sample shows magnetic hysteresis at room temperature, with a coercivity of 1330 Oe, indicating that the sample is not antiferromagnetic. Coercivity of the sample is larger than that reported by Park *et al.* (425 Oe) (Ref. 13) for particles of similar size (51 nm) synthesized by a different method. Similarly, the exchange field,  $H_{ex} = (H_{c1} - H_{c2})/2$ , is also much larger in the present case (125 Oe when compared to 25 Oe). These results suggest that the magnetic characteristics of the nanoparticles of the material are depending on the method of synthesis which determine the surface characteristics. The origin of the higher magnetic moment for BiFeO<sub>3</sub> nanoparticles is attributed to surface contribution.<sup>13</sup> For BF650, the  $M-H$  curve recorded at 10 K (inset of Fig. 5) indicates very weak ferromagnetism with a coercivity of 75 Oe.

Various parameters derived from the magnetic hysteresis curves are shown in Fig. 6. There are some interesting observations from the temperature dependence coercivity ( $H_c$ ),

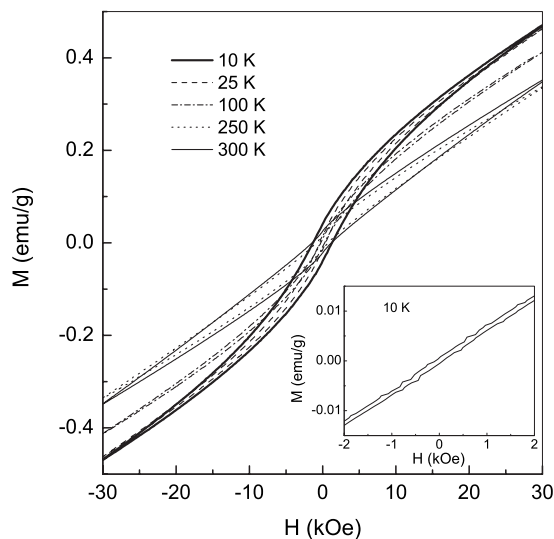


FIG. 5. Magnetic hysteresis loops of BF500 recorded at different temperatures. Inset:  $M-H$  behavior of BF650 at 10 K.

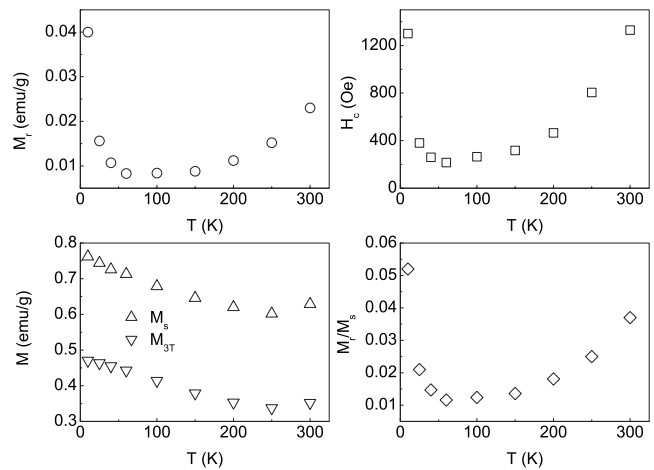


FIG. 6. Coercivity ( $H_c$ ), remnant magnetization ( $M_r$ ), magnetization at 30 kOe ( $M_{3T}$ ), saturation magnetization ( $M_s$ ), and the ratio  $M_r/M_s$  of BF500 as a function of temperature.

remanent magnetization ( $M_r$ ), and saturation magnetization ( $M_s$ ). There is a large drop in the coercivity as the temperature is decreased down to 200 K. The coercivity then remains almost constant with a minimum at  $\sim 50$  K and increases to a large value below 30 K as the temperature is decreased. Similar characteristics are observed in the case of the remnant magnetization and  $M_r/M_s$  ratio also. On the other hand, the magnetization at 3 T (maximum field used for measurement) as well as the saturation magnetization show a minimum at  $\sim 250$  K and increase continuously as the temperature is decreased down to 10 K.

Figure 7 shows a comparison of the FC and ZFC magnetization curves of BF500 and BF650, measured under normal and different conditions. Apart from the normal FC and ZFC measurements, the field-cooled and zero-field-cooled magnetization measurements were also carried out after applying a large field and then degaussing the sample at the lowest temperature. Such measurements clearly give evidence for the contribution from domain pinning effects.<sup>15,16</sup> The sample was initially cooled from room temperature to 10 K in zero external magnetic field. At the lowest temperature, a large magnetic field of 10 kOe was applied. The magnetic field was then reduced to zero and the sample was then degaussed at 10 K. After the remnant magnetization was reduced to zero by degaussing at 10 K, the sample's magnetization was recorded while warming in a field of 500 Oe as in the case of the usual ZFC magnetization measurement. The same experiment was repeated after cooling the sample in a field of 500 Oe as in the case of normal FC measurements. Similar measurements were repeated after cooling the sample under FC and ZFC conditions to 28 K, a temperature slightly above 22 K where a minimum is observed in the FC magnetization measurements.

For BF500, after applying a field and degaussing at 10 K, the ZFC magnetization curve [curve ZFC1 in Fig. 7(a)] shows a large drop in the magnetization up to 20 K and the rest of the features are the same as in the normal ZFC curve. However, the magnetization is larger at all temperatures and a larger increasing difference is observed above  $\sim 100$  K so that the room-temperature value is much larger than that for

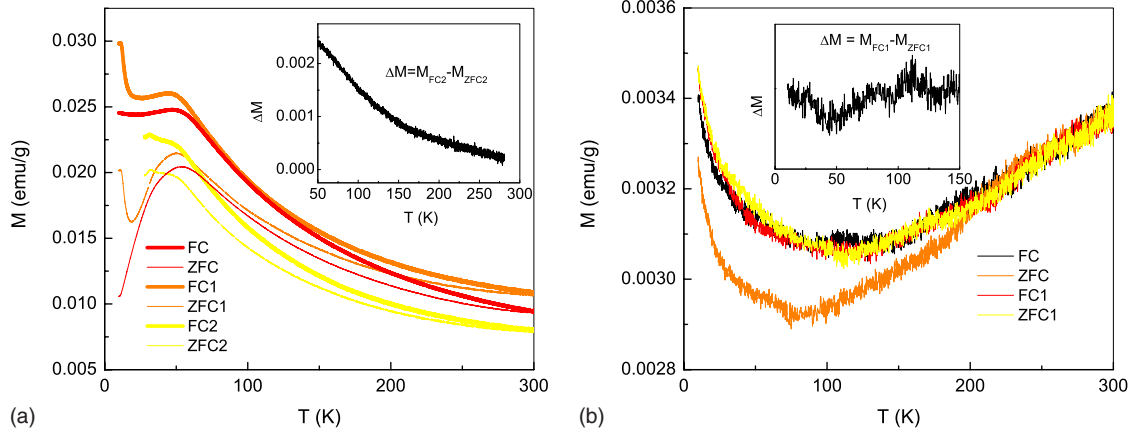


FIG. 7. (Color online) Comparison of the ZFC and FC magnetization curves of (a) BF500 and (b) BF650, measured under different conditions as described in the text.

the virgin sample. Similar features are observed in the case of the FC magnetization [curve FC1 in Fig. 7(a)] also. Here, the minimum is shifted to 26 K and the magnetization shows larger difference above  $\sim 140$  K. Both the new FC and ZFC curves show a maximum at  $\sim 50$  K. On the other hand, when the sample is cooled down to 28 K only, during the FC and ZFC measurements, the natures of both FC and ZFC magnetization curves [curves FC2 and ZFC2 in Fig. 7(a)] are almost identical after degaussing. In this case, only a shoulder is observed at 50 K in the magnetization curves. This indicates that the maximum observed at 50 K in the normal FC or ZFC curve is not associated with any spin-glass-like transition or phase transition. Also, the magnetization at 300 K is lower than that of the virgin sample. The difference between  $M_{FC2}$  and  $M_{ZFC2}$  [inset of Fig. 7(a)] shows a larger slope change around 140 K, indicating a possible change in the domain structure of the material at this temperature. For BF650, after degaussing at 10 K, there is not much difference between the FC and ZFC curves [curves FC1 and ZFC1 in Fig. 7(b)]. Both curves show a minimum at 110 K, slight deviation below 100 K, and again overlapping below 25 K. This may be clearly seen from the difference between  $M_{FC1}$  and  $M_{ZFC1}$  [inset of Fig. 7(b)] which shows a minimum at 50 K.

Previous studies on BiFeO<sub>3</sub> single crystals showed a sharp decrease in the magnetization in both the FC and ZFC curves up to 30 K.<sup>6</sup> ac susceptibility studies indicated a frequency-dependent cusp at 29 K assigned to spin-glass nature and weak ferromagnetism. From the present results, it appears that the large decrease in the FC magnetization up to 25 K as the temperature is increased, for both BF500 and BF650, is due to some changes in the magnetic anisotropy or domain pinning behavior of the system which can also show frequency dependence in the ac susceptibility. The effect of pinned domain walls is expected to reflect in the coercivity of the material<sup>16</sup> and this is observed as a large decrease in the coercivity up to 30 K.

A sharp cusp in the ZFC curve at 50 K is assigned to a superparamagnetic blocking of the spins.<sup>6</sup> Recent studies on (111) oriented thin film of BiFeO<sub>3</sub> showed that the maximum at 50 K is field dependent and varies according to the well-known de Almeida–Thouless (AT) line where the freezing

temperature  $T_f \propto H^{2/3}$  suggesting an acentric long-range spin-glass behavior and mean-field system.<sup>7</sup> The AT line deviates above 140 K and this temperature corresponds to the temperature at which the magnon cross section diverges. However, it has been concluded that the AT behavior is not a proof for the spin-glass behavior as it can be due to superparamagnetism as well as domain pinning effects. Park *et al.* showed that a maximum in the magnetization is observed at this temperature for samples of all sizes, bulk, as well as nanoparticles.<sup>13</sup> This suggests that the feature at 50 K is an intrinsic property of BiFeO<sub>3</sub>. Present results show that the coercivity is minimum at this temperature for BF500 and the maximum at 50 K in the ZFC and FC curves can be suppressed after degaussing the sample at a lower temperature, indicating that this feature also is due to some domain pinning behavior. The shape of the ZFC magnetization curve when measured in a low magnetic field is related to the magnitude and temperature variation of the coercivity which is a measure of the anisotropy.<sup>17</sup> Thus, there is a direct correlation between the shape of the ZFC magnetization curve and the domain structure of a material. The inverse of the coercivity of BF500, normalized with respect to the maximum in the ZFC magnetization, is compared in Fig. 3. The features of both curves are comparable at low temperatures. Although there is no strong magnetic feature for BF500 at 100 K corresponding to the minimum observed in the FC and ZFC curves for BF650 after degaussing, a minimum in the remanence is observed at 100 K for BF500.

A broad minimum is observed around 150 K in the FC and ZFC measurements on single crystals.<sup>6</sup> A ferromagnetic transition is observed at this temperature from studies on oriented thin films.<sup>8</sup> The present results show that this is not a true ferromagnetic transition. No indication for such a magnetic transition is observed from studies on BF500, except that (i) a large deviation in the inverse of the coercivity is observed above 150 K, (ii) a slope change in this temperature region is observed in the difference between FC and ZFC magnetizations after degaussing of BF500, and (iii) the coercivity shoots up above this temperature. These facts again suggest the correlation between the magnetic characteristics and the domain structure of the material. The divergence between FC and ZFC magnetization curves of single



crystalline BiFeO<sub>3</sub> below 250 K is previously assigned to spin-glass behavior.<sup>6</sup> A similar feature is observed for the larger particles of BiFeO<sub>3</sub> (BF650) in the present work. However, this divergence between FC and ZFC is observed immediately below the magnetic transition temperature (~630 K) for the smaller particles (BF500), similar to other ferromagnetic systems. A minimum in the saturation magnetization is observed around 250 K for BF500, indicating that the divergence between FC and ZFC curves for BF650 below 230 K is not a true spin-glass behavior. For larger particles, this can be due to the strong coupling between the antiferromagnetic and ferroelectric domain structures.

#### IV. CONCLUSIONS

For nanoparticles of BiFeO<sub>3</sub> of two different sizes, anomalous magnetic characteristics are observed at temperature regions closer to that of the phase transitions reported at 90, 140, 200, and 250 K from Raman spectroscopic studies and spin-glass-like transitions reported at 30, 50, 150, and

250 K from magnetic studies on single crystals and thin films. Some changes in the magnetic characteristics are observed at these temperatures when the measurements are done under different experimental conditions, suggesting that the phase transitions or spin-glass-like transitions are directly associated with changes in the intrinsic magnetic nature of the BiFeO<sub>3</sub>, strongly coupled with the lattice. The phase transitions observed in the Raman spectroscopic studies are not directly observed in the magnetic measurements, indicating that these are not dominant magnetic transitions as suggested. Similarly, there cannot be many spin-glass-like transitions in the same material, as reported. Hence, the anomalies observed at the specified temperatures are likely to be some changes associated with the domain structure of the material at low temperatures.

#### ACKNOWLEDGMENTS

S.V. and M.B.M. are grateful to CSIR, India, for financial assistance.

\*pa.joy@ncl.res.in

<sup>1</sup>H. Bea, M. Gajek, M. Bibes, and A. Barthelemy, *J. Phys.: Condens. Matter* **20**, 434221 (2008).

<sup>2</sup>S. M. Selbach, T. Tybell, M.-A. Einarsrud, and T. Grande, *Adv. Mater. (Weinheim, Ger.)* **20**, 3692 (2008).

<sup>3</sup>J. M. Moreau, C. Michel, R. Gerson, and W. J. James, *J. Phys. Chem. Solids* **32**, 1315 (1971).

<sup>4</sup>R. Przenioslo, A. Palewicz, M. Regulski, I. Sosnowska, R. M. Ibberson, and K. S. Knight, *J. Phys.: Condens. Matter* **18**, 2069 (2006).

<sup>5</sup>A. Palewicz, T. Szumiata, R. Przenioslo, I. Sosnowska, and I. Margiolaki, *Solid State Commun.* **140**, 359 (2006).

<sup>6</sup>M. K. Singh, W. Prellier, M. P. Singh, R. S. Katiyar, and J. F. Scott, *Phys. Rev. B* **77**, 144403 (2008).

<sup>7</sup>M. K. Singh, R. S. Katiyar, W. Prellier, and J. F. Scott, *J. Phys.: Condens. Matter* **21**, 042202 (2009).

<sup>8</sup>R. Palai, H. Huhtinen, R. S. Katiyar, and J. F. Scott, arXiv:0707.1657 (unpublished).

<sup>9</sup>M. Cazayous, Y. Gallais, A. Sacuto, R. de Sousa, D. Lebeugle, and D. Colson, *Phys. Rev. Lett.* **101**, 037601 (2008).

<sup>10</sup>J. F. Scott, M. K. Singh, and R. S. Katiyar, *J. Phys.: Condens. Matter* **20**, 322203 (2008).

<sup>11</sup>S. A. T. Redfern, C. Wang, J. W. Hong, G. Catalan, and J. F. Scott, *J. Phys.: Condens. Matter* **20**, 452205 (2008).

<sup>12</sup>R. Mazumder, P. S. Devi, D. Bhattacharya, P. Choudhury, A. Sen, and M. Raja, *Appl. Phys. Lett.* **91**, 062510 (2007).

<sup>13</sup>T. J. Park, G. C. Papaefthymiou, A. J. Viescas, A. R. Moodenbaugh, and S. S. Wong, *Nano Lett.* **7**, 766 (2007).

<sup>14</sup>P. A. Joy and S. K. Date, *J. Magn. Magn. Mater.* **222**, 33 (2000).

<sup>15</sup>P. A. Joy and S. K. Date, *J. Magn. Magn. Mater.* **218**, 229 (2000).

<sup>16</sup>C. R. Sankar and P. A. Joy, *Phys. Rev. B* **72**, 024405 (2005).

<sup>17</sup>P. A. Joy and S. K. Date, *J. Magn. Magn. Mater.* **220**, 106 (2000).